This is to certify that the

thesis entitled

DIENCEPHALIC PROJECTIONS FROM THE ROSTRAL AND CAUDAL PARTS OF THE DORSAL COLUMN NUCLEI IN THE RAT

presented by

Anthony Constantin Bonduki

has been accepted towards fulfillment
of the requirements for

Ph. D. degree in Psychology and Neuroscience

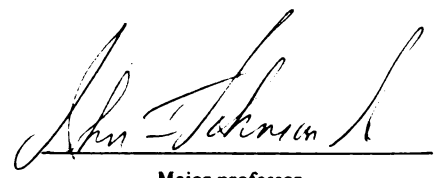

Major professor
John I. Johnson Jr.

9 August 1977
Date

O-7639

DIENCEPHALIC PROJECTIONS FROM THE ROSTRAL AND CAUDAL PARTS OF THE DORSAL COLUMN NUCLEI IN THE RAT

By

Anthony Constantin Bonduki

A DISSERTATION

Submitted to
Michigan State University
in partial fulfillment of the requirements
for the degree of

DOCTOR OF PHILOSOPHY

Department of Psychology and Neurosciences Program

1977

ABSTRACT

DIENCEPHALIC PROJECTIONS FROM THE ROSTRAL AND CAUDAL PARTS OF THE DORSAL COLUMN NUCLEI IN THE RAT

By

Anthony Constantin Bonduki

Although a number of regions in the thalamus and subthalamus have been reported to receive projections from the dorsal column nuclei (DCN), there is no agreement in the literature over the number, identity, and location of such regions. There are also specific disagreements as to whether the rostral regions of the DCN project to the same diencephalic targets as do the caudal regions of the DCN (Hand and Liu: Anat. Rec., '66, 154, 353-354; Lund and Webster: J. Comp. Neur., '67, 130, 301-312; Boivie: Brain Res., '71, 28, 459-490; RoBards and Watkins: Neurosci. Abstracts, '75, 1, 215; Hand and Van Winkle, '77, 171, 83-109). The present study was carried out in order to identify the diencephalic DCN targets in the rat, and to assess the possible differences in diencephalic projections between rostral and caudal parts of the DCN.

Lesions were made in the DCN of albino rats, rostral to the obex, caudal to it, and encroaching on both parts or involving their entire rostro - caudal extent. Control cases included eye removals, and sham DCN lesions. Spinal hemisections at C_3-C_4 were also made. Following survivals of two to nine days, the animals were perfused

and the brains were processed according to the Fink-Heimer method for anterograde degeneration. Terminal degeneration in the thalamus and subthalamus was charted over projected drawings of the sections, and counts were made of the silver grains of degenerating terminals in five observed target regions and in four adjacent non-targets, both contralateral and ipsilateral to the lesion. Those counts were cross-checked by independent "judges." The data from the counts was then subjected to a series of analyses of variance and multiple comparisons tests (SNKL).

The quantitative results indicated that: 1) the number of degenerating terminals was 1035 percent higher on the side contralateral to the DCN lesion than on the ipsilateral side ($p < .001$). 2) The number of degenerating terminals was 1021 percent higher in the DCN lesion groups than in the control group ($p < .05$), and 151 percent higher in the entire DCN lesion group than in the rostral and the caudal DCN lesion groups ($p < .05$). 3) Three subsets of nuclei on the contralateral side were different from each other ($p < .05$): a ventrobasal complex (lateral part: VB_l) subset containing the highest amount of degeneration: 193 percent higher than in the extra-VB target nuclei and 1145 percent higher than in the non-target nuclei; the second subset was composed of extra-VB target nuclei: nucleus angularis (M. Rose: Mém. de l' Acad. Pol. des Sci. et Lett., Cracovie, sér. B, '35, 1-108; Mehler: Ann. N. Y. Acad. Sci., '69, 167, 424-468), the anterior pretectal nucleus, the magnocellular division of the medial geniculate body, and the ventral part of the zona incerta;

degenerating terminals in the nuclei of this subset were 594 percent more numerous than in the non-target nuclei; and the third subset consisted of non-targets: the medial geniculate body, the optic/superficial gray strata of the superior colliculus, the medial part of the ventrobassal complex, and the dorsal part of the zona incerta. A DCN projection to the anterior pretectal nucleus in the rat has been described by Lund and Webster ('67, op. cit.) in its ventral subdivision only; in the present study, terminals were present throughout its dorso-ventral extent; however, only the caudal part of the nucleus as described by Scalia (J. Comp. Neur., '72, 145, 223-258), received DCN projections. Lund and Webster ('67, op. cit.) also described projections to the lateral part of the zona incerta; our results, in agreement with Smith (J. Comp. Neur., '73, 148, 423-446), found them in its ventral part. A spinal projection to VB_1 was confined to its rostral third, overlapping there with DCN terminals; this projection was ipsilateral only. Similar results were obtained by Lund and Webster (J. Comp. Neur., '67, 130, 313-328) and Mehler ('69, op. cit.).

The target nuclei in the thalamus and subthalamus were the same for the projections from the rostral and the caudal parts of the DCN, and no differences were detected in the amounts of degeneration ($p > .05$). Also, the antero-posterior, dorso-ventral, and medio-lateral extents of terminal degeneration within those nuclei were almost identical for rostral and caudal lesions. Contrary to a previous report (Hand and Van Winkle, '77, op. cit.), the amount of degeneration in VB_1 too was similar in rostral and caudal DCN cases.

This dissertation is dedicated to my parents and to my wife Marilou; their sacrifices for me have been immeasurable.

ACKNOWLEDGMENTS

I would like to express my deep affection and gratitude to my professor, Dr. John I. Johnson, Jr. He patiently provided me with guidance and support, and always come to the rescue when needed. I also extend my appreciation to the other members of my committee, Dr. Martin Balaban, Dr. Glenn Hatton, and Dr. Charles Tweedle, for their guidance and understanding.

I am also ever grateful to my teacher and friend, Professor Mustapha Ziwar who guided my steps during my undergraduate years, Dr. Venonika Grimm who introduced me to neuropsychology, Dr. Thomas Jenkins who introduced me to neuroanatomy, and Dr. Charles R. R. Watson who helped me master the silver-impregnation method used in this study.

Neal Brophy and Satchel Garrison assisted with the photography, and Michael Peterson with the histological processing of the tissue blocks containing the lesions. Ray R. Humphrys generously offered time and assistance with the statistical analysis of the data. Ms. Adeline Zimmerman plowed through the handwritten manuscript and typed its original draft. Those contributions are gratefully acknowledged.

This research was supported by grants NS05982 and RR07049 from NIH, and GB43236 from NSF, and funds from the Department of Psychology, Michigan State University.

TABLE OF CONTENTS

	Page
LIST OF TABLES	vi
LIST OF FIGURES	vii
LIST OF ABBREVIATIONS	viii
INTRODUCTION	1
MATERIALS AND METHODS	3
Subjects	3
Surgery	3
Controls	4
Histological Processing	4
Analysis of the Data	5
RESULTS	11
Pattern of Projections	11
Quantitative Results	21
DISCUSSION	24
Quantitative Treatment of the Data	24
Diencephalic Target Nuclei of DCN Projections	29
Ventrobasal Complex	29
Zona Incerta	31
Review of the "PO" Region	32
Nucleus Angularis	34
Anterior Pretectal Nucleus	38
Magnocellular Division of the Medial Geniculate	42
Ipsilateral Degeneration	43
Other Nuclei	44
Rostral and Caudal DCN Comparisons	44
Cytoarchitecture	44
Afferents	45
Dorsal Roots Distribution	46
Peripheral Receptive Fields	46
Efferents	47
Overview of Rostral and Caudal DCN Differences	48

Page

BIBLIOGRAPHY 51

APPENDICES 59

A. Fink-Heimer Technique 60

B. Instructions for Counting Terminal Degeneration . . 63

C. Counts of "Grains" of Terminal Degeneration: Tables . 65

LIST OF TABLES

Table		Page
C1.	Counts of silver grains of terminal degeneration in nine diencephalic nuclei resulting from rostral DCN lesions, caudal DCN lesions, entire DCN, and mixed rostral and caudal DCN lesions, and control lesions .	66

LIST OF FIGURES

Figure		Page
1.	Thionine stained sections, and diagrams, through different levels of a rostral DCN lesion ($RDCN_{34}$) . .	6
2.	Thionine stained sections, and diagrams, through different levels of a caudal DCN lesion ($RDCN_{53}$) . .	8
3.	Photomicrographs of sections stained according to the Fink-Heimer method, showing anterograde degeneration in diencephalic target nuclei, and control cases . . .	12
4.	Camera lucida drawings of sections from the diencephalon, showing the extent of terminal degeneration	16
5.	Schematized representation of the terminal degeneration in the target nuclei along the antero-posterior, and the medio-lateral axes of the diencephalon	19
6.	Density of terminal degeneration plotted as a total number of silver grains in a volume of tissue, from each of nine contralateral nuclei	25
7.	Density of terminal degeneration plotted as a total number of silver grains in a volume of tissue, from each of nine ipsilateral nuclei	27
8.	Coronal section through the diencephalon of the rat, at a level corresponding to level E (to F) of Figure 4; thionine stain	37
9.	Coronal section through the diencephalon of the rat, at a level corresponding to level K of Figure 4; thionine stain	39

LIST OF ABBREVIATIONS

Ang,	nucleus angularis
Ant.Pt,	anterior pretectal nucleus
CIN,	central intralaminar nucleus (Killackey and Ebner, '72)
CL,	central lateral nucleus
CP,	cerebral peduncle
DCN,	dorsal column nuclei (cuneate and gracile nuclei)
FR,	fasciculus retroflexus
LCN,	lateral cervical nucleus
LP,	nucleus lateralis posterior
LPL,	posterolateral nucleus, pars lateralis (Lund and Webster, '67a and b)
MGB,	medial geniculate body
MG_{mc},	medial geniculate body, pars magnocellularis; also MG_m: medial division of MGB; MG_i^m: internal division of MGB
ML,	medial lemniscus
OT,	optic tract
Pf,	parafascicular nucleus
PO,	posterior region, or posterior group: PO_m, PO_l, PO_i: medial, lateral, and intermediate divisions respectively. PO_p: posterior part of PO (Berkley, '73)
R,	nucleus reticularis thalami
SB,	subthalamic nucleus
SC,	superior colliculus
Sg,	suprageniculate nucleus
SN_c,	substantia nigra, pars compacta
SN_r,	substantia nigra, pars reticulata
VB_l,	ventrobasal complex, pars lateralis; also VPL: ventral posterolateral nucleus
VB_m,	ventrobasal complex, pars medialis
ZI_d^m,	zona incerta, dorsal part
ZI_v,	zona incerta, ventral part

INTRODUCTION

A number of nuclei in the thalamus and subthalamus have been identified as recipients of projections from the dorsal column nuclei (DCN: cuneate and gracile nuclei) in a variety of species: opossum (Hazlett et al., '72; RoBards and Watkins, '75), hedgehog (Jane and Schroeder, '71), tree shrew (Schroeder and Jane, '71), rat (Lund and Webster, '67a), cat (Hand and Liu, '66; Boivie, '71a; Jones and Powell, '71; Jones and Burton, '74; Hand and Van Winkle, '77), and macaque monkey (Bowsher, '61). There is a general consensus over the connection to the ventrobasal complex (VB), but not over the "extra-VB" nuclei. These have included a central intralaminar nucleus (CIN), the magnocellular division of the medial geniculate, (MG_{mc}), the parafascicular nucleus (Pf), a posterior thalamic nucleus, a pretectal nucleus, the suprageniculate nucleus (Sg), the zona incerta (ZI), and a "PO group" which inconsistently includes some of these areas. Moreover, Groenewegen et al., ('75) could ascertain a projection only to VB in the cat; and Basbaum et al., ('77) did not find any DCN labeling folloiwng HRP injections in a "posterior group" in the thalamus of the rat.

Differences in cytoarchitecture have been reported between various regions of the DCN rostral and caudal to the obex (Kuypers and Tuerk, '64; Basbaum and Hand, '73). The differences were

reported to be correlated with the sites of termination in the DCN, of corticofugal afferents (Kuypers and Tuerk, '64), and of primary afferents from the dorsal funiculus, and of non-primary afferents ascending in the dorsal and in the dorsolateral funiculi (Tomasulo and Emmers, '72; Rustioni, '73 and '74; Nijensohn and Kerr, '75). They have also been reported to correspond to different patterns of projections to the thalamus and subthalamus from various portions of the DCN in the cat: rostral and middle portions (Hand and Liu, '66); rostral and caudo-ventral, and caudo-dorsal portions (Hand and Van Winkle, '77); and from rostral and caudal parts in the DCN of the rat (Lund and Webster, '67a). However, Boivie ('71a) did not find any difference in projections between rostral and caudal DCN in the cat, and RoBards and Watkins ('75) reported similar projections from different regions along the rostro-caudal extent of the DCN in the opossum.

The purpose of this investigation is 1) to identify the various diencephalic nuclei receiving projections from the dorsal column nuclei in the rat; 2) their relation to a "PO region" in the thalamus; and 3) to investigate the possible differences in diencephalic projections from the rostral and caudal parts of the DCN.

MATERIALS AND METHODS

Subjects

Seventy-eight albino rats from the Sprague-Dawley strain were used in this investigation. They were from both sexes, four to ten months old, and weighed 250 to 350 gm.

Surgery

Unilateral lesions (sixty seven) were made in different parts of the dorsal column nuclei: rostral to the obex, caudal to the obex, encroaching on both rostral and caudal portions (mixed), and including the entire rostro-caudal extent of the DCN.

Surgery was done under ether anesthesia; a cylindrical cushion was placed under the animal's throat to permit a flexure of the head in an antero-ventral direction. A longitudinal incision of the skin was then made along the midline of the back, the muscles were separated and retracted, and the dura over the foramen magnum was cut and reflected. A portion of the occipital bone was removed in rostral DCN, entire DCN, and sham lesions, but not in caudal DCN lesions. The lesions were done under an Olympus operating microscope; they were made with suction, or with a scalpel, or electrolytically with 200-500 μA for 10-15 secs. through a glass-insulated tungsten microelectrode as anode which had a 60 μm uninsulated tip length. Following the lesion, absorbable gelatin sponge (Gelfoam)

was applied, the wound was closed, the skin sutured, and the animal was given an IP injection of dextrose (10-15cc).

Controls

Controls included sham DCN lesions in three animals, unilateral eye removals in three rats, and cervical spinal hemisections in nine. Eye removals were made by gently pulling the eye out of the socket, and severing the ocular muscles and the optic nerve. Spinal hemisections were done at the level of C_3-C_4; the vertebral column was exposed, a laminectomy made, the dura reflected, and the cord was crushed with microforceps for 15 to 20 secs. or was cut with a scalpel.

Histological Processing

Following a survival period of 2 to 9 days, the animals were perfused with 0.9% saline followed by 10% formalin, the brains were extracted and sectioned frozen at 33 μm thickness in a coronal plane. Every tenth section (or fith in a few cases) was stained according to the Fink-Heimer technique, procedure I (Fink and Heimer, '67; Heimer, '70) for tracing degeneration (Appendix A). Adjacent sections were stained with thionine for cytoarchitectonic localization. A block from the medulla or from the cord containing the lesion was embedded in celloidin, cut coronally at 25 μm and every fifth section was stained with thionine to assess the extent of the damage. Adjacent cord sections were also stained with luxol-blue.

Analysis of the Data

Sections from four rostral (Figure 1), five caudal (Figure 2), and ten entire and mixed DCN lesions and from five spinal hemisections, three eye removals, and two sham DCN lesions were examined with the light microscope. Terminal degeneration was charted on projected drawings.

The results were also quantified in two rostral lesions, two caudal lesions, two both rostral and caudal (one entire DCN, and one mixed), and two control (one eye removal, and one sham DCN) lesions. Animals with 3 to 5 days survivals were selected where terminal degeneration was at an optimum level in all the nuclei. Counts of "grains" of terminal degeneration were made under oil immersion (objective x 40) in 5 identified target nuclei and in 4 adjacent non-target nuclei, both contra- and ipsilateral to the lesion, and in the contralateral target nuclei the counts were done on two consecutive sections (300-330 μm apart). In each nucleus of each section counts of terminal degeneration "grains" were done in six squares chosen randomly from a total of sixteen squares in one quadrant of a Whipple-Hausser ocular micrometer. The random selection was obtained by taking the last two digits from six consecutive entries in a table of random numbers; the digit before last was considered 0 (zero) when even, and 1 (one) when odd. Duplicate numbers and numbers higher than 16 were discarded. Counts made on the contralateral side of the two rostral cases and the two caudal cases, and in some of the ipsilateral nuclei, were cross-checked by ten independent judges unfamiliar with the Fink-Heimer procedure and unaware

Figure 1. Left column: thionine stained sections through different levels of a rostral DCN lesion ($RDCN_{34}$). The top photograph represents the most anterior section showing tissue damage, the bottom photograph represents the most posterior level showing tissue damage, and the center photograph is of a section in the middle of the antero-posterior extent of the lesion. Right column: diagrams of the corresponding photographs on the left; damaged region is shaded in black. Scale for all the sections is the same as in the top photograph.

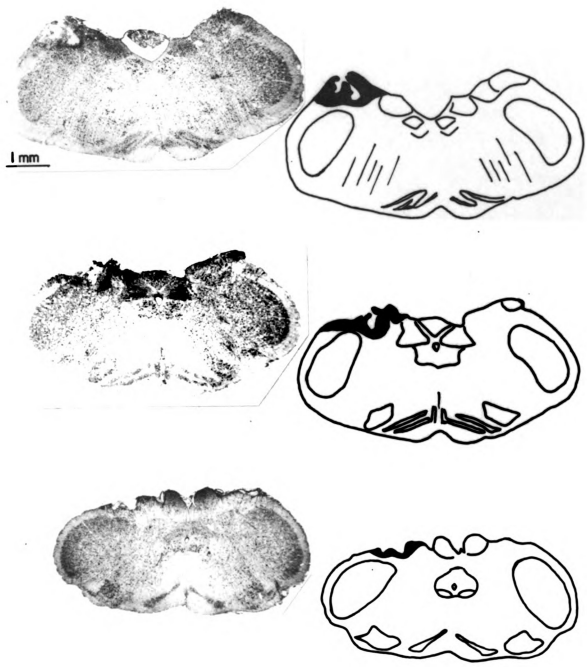

FIGURE 1

Figure 2. Left column: thionine stained sections through different levels of a caudal DCN lesion ($RDCN_{53}$). The sequence of photographs is similar to that of Figure 1. The diagrams in the right column correspond to the adjacent photographs; damaged region is shaded in black. Scale for all the sections is the same as in the top photograph.

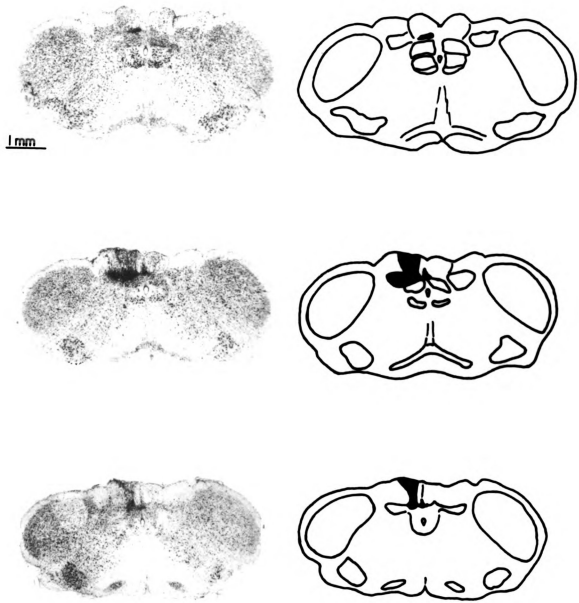

FIGURE 2

of the location where they were counting; they were all given a similar set of instructions (Appendix B). The data from the various counts was subjected to statistical analysis (see Results and Discussion sections).

RESULTS

Pattern of Projections

In all the cases of DCN lesions, terminal degeneration was present on the side contralateral to the lesion (Figure 3), in 1) the lateral part of the ventrobasal complex (VB_l), 2) nucleus angularis (Ang), 3) throughout the dorso-ventral extent of the anterior pretectal nucleus (Ant.Pt), 4) the magnocellular division of the medial geniculate (MG_{mc}), and 5) the ventral portion of the zona incerta (ZI_v).

Apart from slight background staining, no degeneration was observed on the side ipsilateral to the lesion. Ipsilateral terminals were present in all the target nuclei however, when some of the caudal lesions encroached on the other side (Figure 2); and in one animal with a rostral lesion ($RDCN_{34}$), ipsilateral degeneration was observed in Ant.Pt and MG_{mc} only (Figure 7).

The pattern of projections to the diencephalon was similar in all DCN lesions (Figure 3); rostral, caudal, mixed and entire. The same target nuclei were involved, and the rostro-caudal, mediolateral, and dorso-ventral extents of terminal degeneration in each nucleus were almost identical in all the DCN lesion groups (Figures 4 and 5). Figure 4 shows on projected drawings of the sections the various levels of the diencephalon at which terminal degeneration was found. Figure 5 shows a schematized representation of the

Figure 3a. Photomicrographs of sections stained according to the Fink-Heimer method, showing anterograde degeneration in diencephalic target nuclei, and control cases.
A. Photomicrograph from Ang; rostral DCN lesion.
B. Photomicrograph from Ang; caudal DCN lesion.
C. Photomicrograph from Ang; eye removal (control lesion).
D. Photomicrograph from Ant.Pt; rostral DCN lesion
The scale below B is for all the sections.

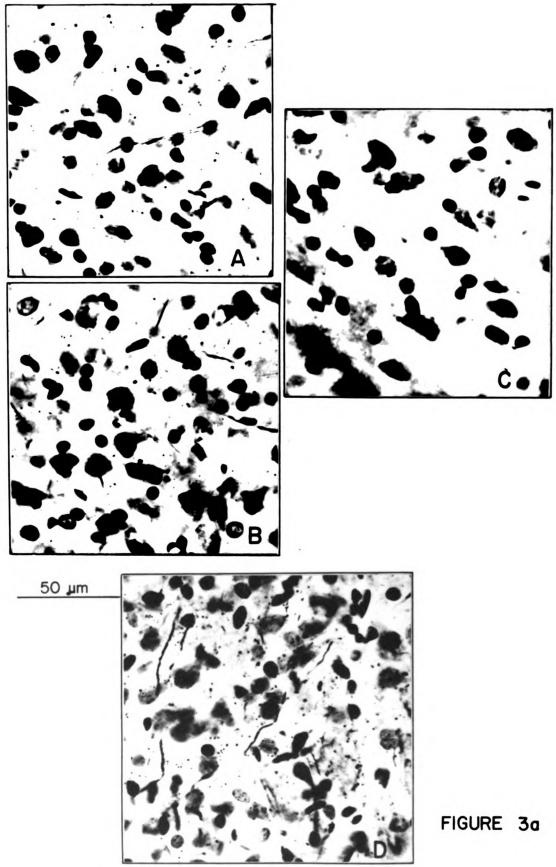

FIGURE 3a

Figure 3b. Photomicrographs of sections stained according to the Fink-Heimer method, showing anterograde degeneration in diencephalic target nuclei, and control cases. Degeneration seen in VB_l (E, F) was denser than that in other nuclear regions.

E. Photomicrograph from VB_l; rostral DCN lesion.
F. Photomicrograph from VB_l; caudal DCN lesion.
G. Photomicrograph from VB_l; sham DCN lesion (control case).
H. Photomicrograph from MG_{mc}; rostral DCN lesion.
I. Photomicrograph from ZI_v; caudal DCN lesion.

Scale is the same as in Figure 3a.

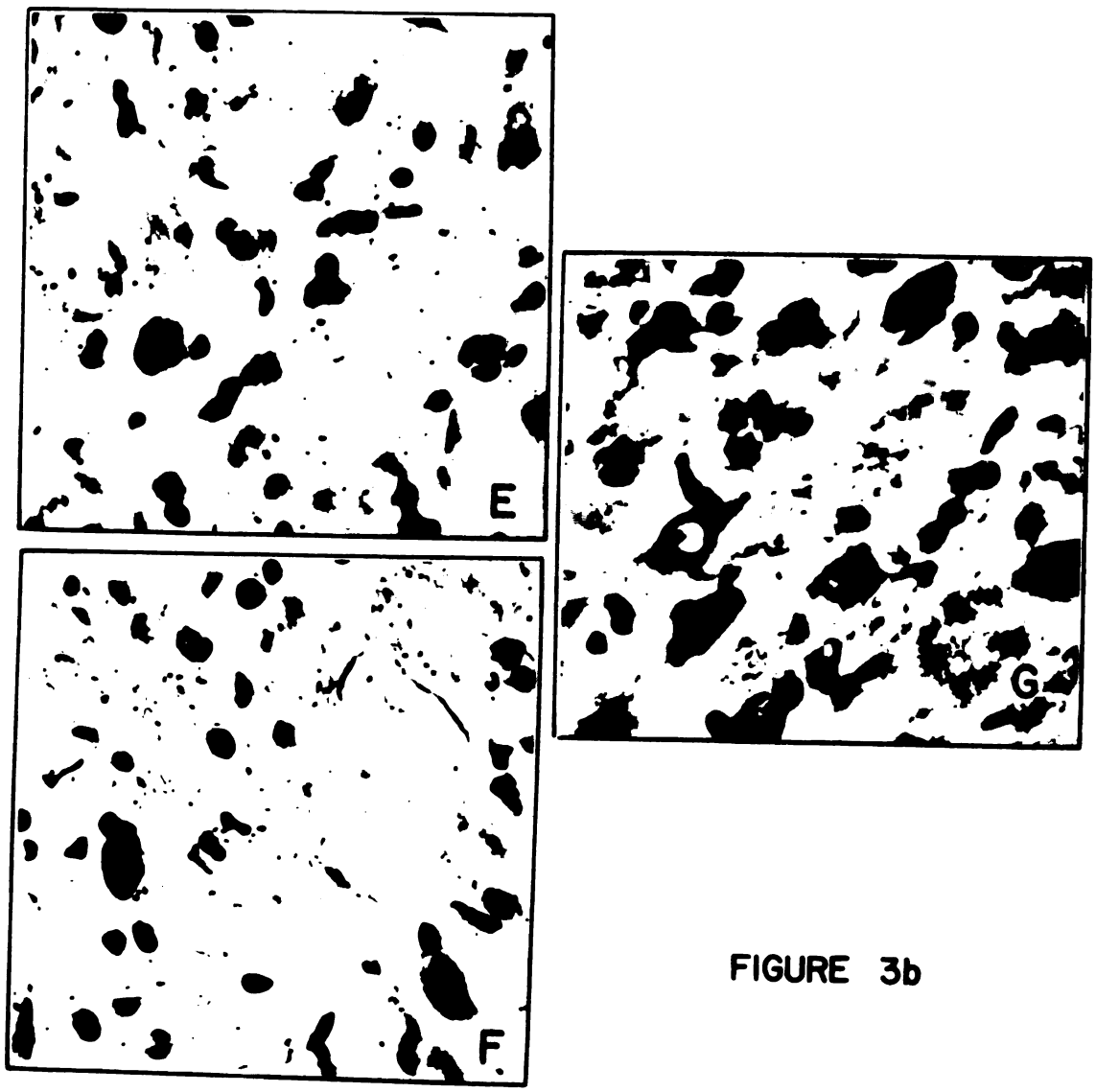

FIGURE 3b

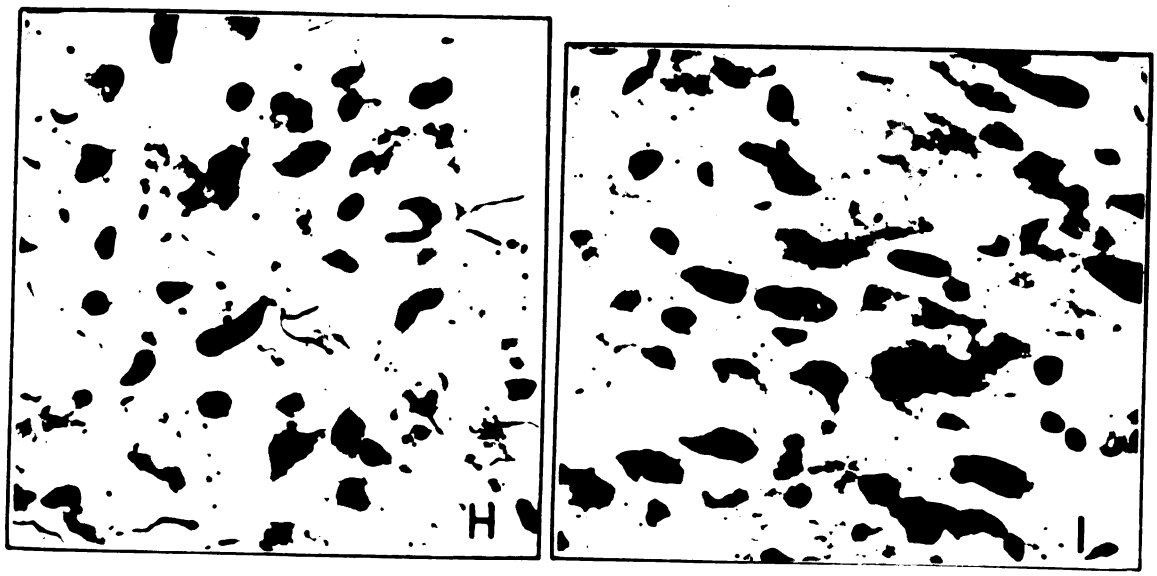

Figure 4. Camera lucida drawings of sections from the diencephalon (A: anterior, M: posterior), showing the extent of terminal degeneration (stippling) from 1) a rostral DCN lesion (R), 2) a caudal DCN lesion (C), and 3) a whole DCN lesion (W). The levels A - M are from sections 330 μm apart.

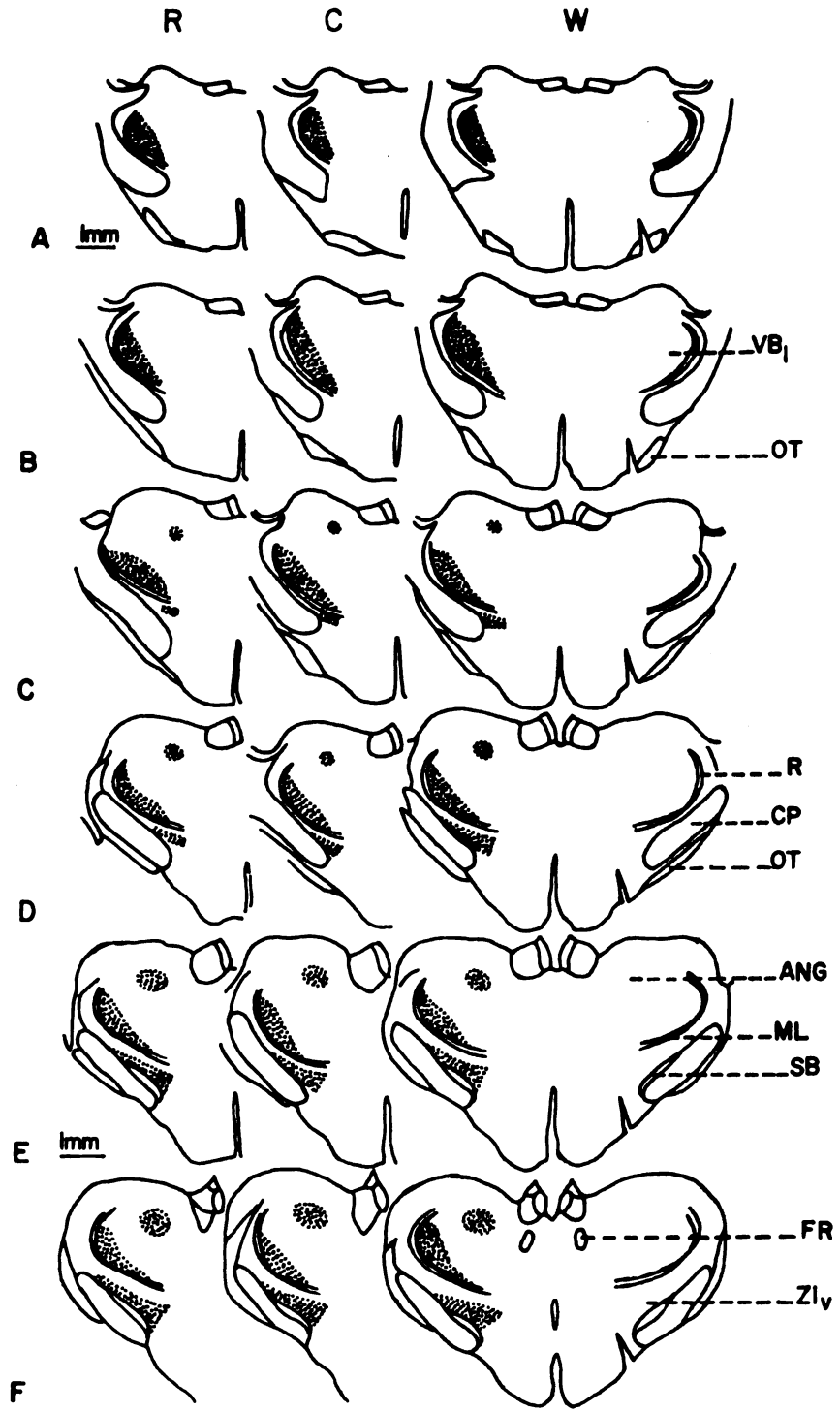

FIGURE 4a

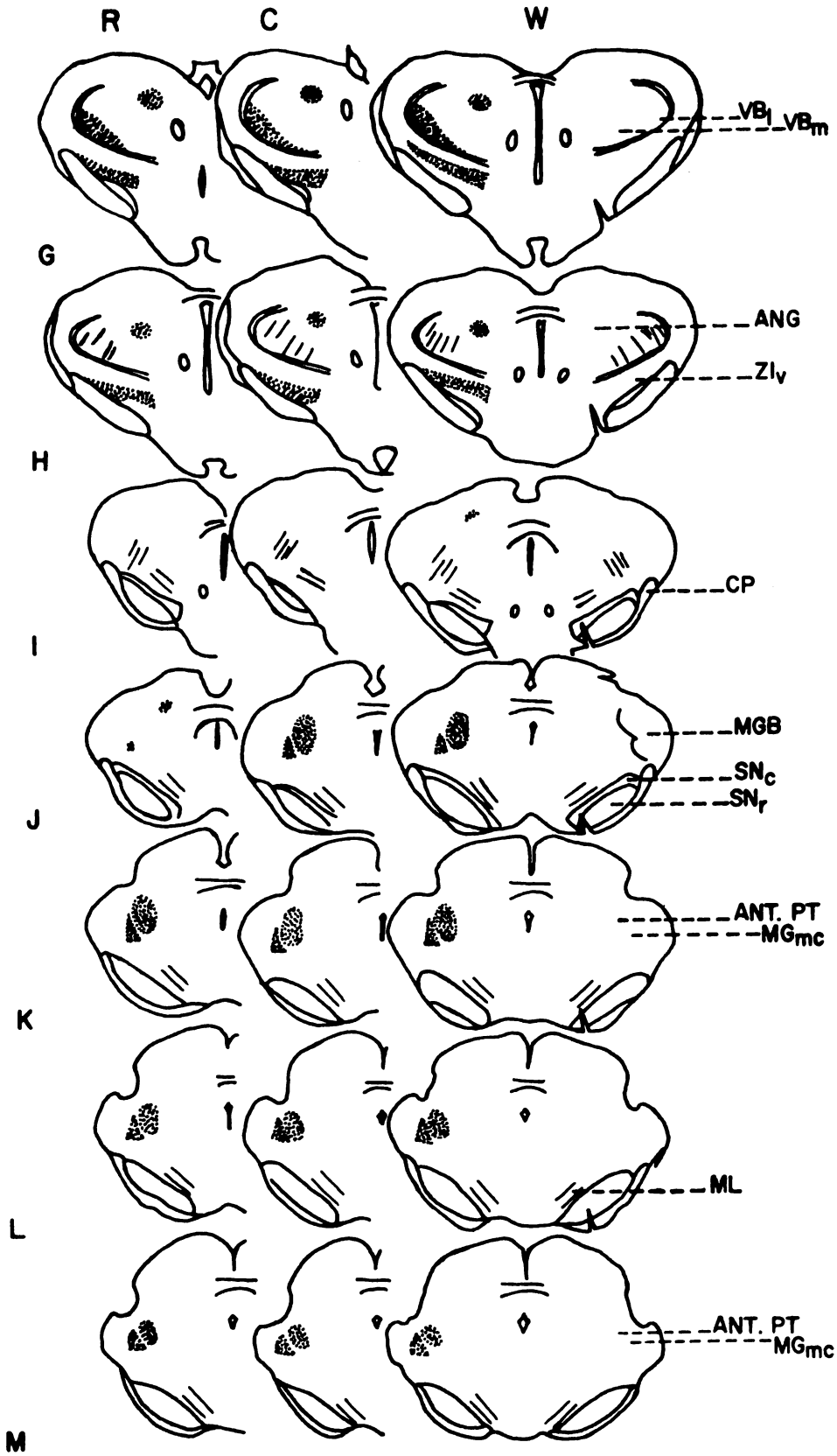
R
C
W
VB$_l$
VB$_m$
G
ANG
ZI$_v$
H
CP
I
MGB
SN$_c$
SN$_r$
J
ANT. PT
MG$_{mc}$
K
ML
L
ANT. PT
MG$_{mc}$
M

FIGURE 4b

Figure 5. Schematized representation of the terminal degeneration in the target nuclei. Degeneration in each nucleus was plotted at its widest extent along the medio-lateral axis of the diencephalon, at successive antero-posterior levels (A-M). The result is a diagrammatic projection on a horizontal section. R, C, W: same as Figure 4. 1 mm = 50 μm.

degeneration in the antero-posterior and medio-lateral axes of the diencephalon. The degeneration extended from level A to level G in VB_l. In nucleus angularis and the zona incerta, it extended from C to H. The terminals in nucleus angularis were slightly more ventral at their caudalmost level (H). In the zona incerta only the ventral portion was involved, and the field of degeneration grew medio-laterally at caudal levels along with the enlargement of the nuclear area of ZI. Degeneration in the anterior pretectal nucleus and in the magnocellular medial geniculate extended from level J to M. A small field of terminals is present at level I in Ant.Pt of the entire DCN case illustrated because it represents a slightly more posterior plane than in the illustrated rostral DCN and caudal DCN cases. Similarly, degeneration is less extensive at level J of Ant.Pt and MG_{mc} in the rostral case illustrated because it is slightly more anterior than its counterparts in the other two cases represented. Both large and smaller cells in MG_{mc} were involved in the field of terminals. The medialmost boundary of MG_{mc} however, is somewhat arbitrary, since its cells large and small are scattered medially among fibers from the medial lemniscus, and terminals get mixed with degenerating fibers.

Quantitative Results

Counts of "grains" of terminal degeneration were made in the five target nuclei (Ang, Ant.Pt, MG_{mc}, VB_l, and ZI_v), and in four adjacent non-target muclei: the ventral division of the medial geniculate body (MGB), the medial part of VB(VB_m), the

optic/superficial gray strata of the superior colliculus (SC), and the dorsal part of ZI (ZI_d). The density of DCN terminals in each of those nine nuclei on the contralateral side is plotted in Figure 6. Counts of "grains" in the ipsilateral nine nuclei are plotted in Figure 7.

Discrepancies between these counts and the counts made by the independent judges did not exceed 9%, with a mode of 2 to 3% in the contralateral target nuclei, and did not exceed one "grain" in the contralateral non-targets (Appendix C).

F_{max} tests for homogeneity of variances (Winer, '62) were computed separately for the group of targets, and the group of non-targets, contralaterally, then ipsilaterally, for each of the lesion cases. The results indicated homogeneity.

In order to determine if any statistical differences were present in the data, a three-factors analysis of variance (lesions x sides x nuclei) with repeated measures on two factors (sides x nuclei), was computed (Winer, '62); all the main effects were significant (p ' s < .001) : sides, F (1,72) = 276.53; lesions, F (3,72) = 67.89; nuclei, F (8,72) = 61.08. Two-way interactions (p < .001) and a 3-way interaction (p < .001) were present.

Differences between the lesion groups were then tested with a two-factors (lesions x nuclei) with repeated measures on one factor (nuclei) analysis of variance. The analysis was made on the contralateral target nuclei in two rostral, two caudal, one entire DCN,

and two control cases.* The result was F (3,34) = 24.68, p < .001 This was followed by multiple comparisons using the Student-Newman-Keuls procedure (SNKL) (Winer, '62), it indicated that:

1. The control group differed from the other three groups (p < .05)
2. the entire DCN case differed from the other three groups (p < .05)
3. the rostral and the caudal groups did not differ from each other (p > .05)

Differences between the nuclei were tested in the same way: a two-factors (lesions x nuclei) with repeated measures on one factor (lesions) analysis of variance was computed for all nine (targets and non-targets) contralateral nuclei on two rostral, two caudal, and two general (one mixed and one entire DCN) cases. The result was F (8,53) = 53.82, p < .001. Three subsets significantly different from each other (p < .05) emerged from the SNKL test: 1) VB_l; 2) extra-VB targets (Ang, Ant.Pt, MG_{mc}, ZI_v); and, 3) non-targets (MGB, Sc, VB_m, ZI_d).

---

*In all analyses of variance, the count of contralateral SC in the eye removal control case (Figure 6) was substituted by zero.

DISCUSSION

Quantitative Treatment of the Data

An initial apprehension at quantifying Fink-Heimer results was not borne out. The procedure proved to be simple and reliable; it does, however, require "clean" sections, relatively free from artifacts such as "dust," and with not too much staining of normal fibers. Also, it is necessary to account for the nuclei being considered when terminal degeneration in each of them is at its optimum.

Three necessary assumptions for computing analyses of variance were met: 1) samples (sampled squares) were drawn at random; 2) variances of the several subgroups (targets, non-targets, on different sides, and in different lesion cases) were homogeneous, as determined by the F_{max} test; and 3) the amount of degeneration in each nucleus was assumed independent from that in the other nuclei.

The interactions obtained in the three-factors analysis of variance may be accounted for by the inclusion of data from nuclei free of terminal degeneration: 1) ipsilateral target and non-target nuclei in all cases; 2) contralateral non-target nuclei in the DCN lesion cases; and 3) contralateral target and non-target nuclei in the control cases.

Degeneration resulting from either rostral or caudal DCN lesions may be considered "moderate" in the extra-VB target nuclei and "heavy" in VB; that resulting from entire DCN lesions may be

Figure 6. Density of terminal degeneration plotted as total number of silver grains in a volume of tissue (10^3 x 5.5 μm^3), from each of nine contralateral nuclei. R and r: rostral DCN lesions; C and c: caudal DCN lesions; M: mixed lesion (partial rostral and caudal); W: entire DCN lesion; E: eye removal (control); S: sham DCN lesion (control).

The different groups identified by the analyses of variance and the multiple comparisons tests (SNKL) may be visualized in Figures 6 and 7: 1) at the bottom of the graphs rest the contralateral non-target nuclei, the nine ipsilateral nuclei, and all the nuclei (both sides) in the control cases (except for contralateral SC in the eye removal case). Then 2) at a high level come the contralateral extra-VB target nuclei (Ang, Ant.Pt, MG_{mc}, ZI_v) in the lesion cases, they overlap with each other in density of terminals so that they all fall in one category of density. No difference appears between caudal and rostral cases either since they are very close to each other and they overlap in all the nuclei. Next, 3) at a higher level, degeneration in VB_l from rostral and caudal lesions forms a special subgroup, with caudal and rostral again overlapping. 4) Projections from the entire DCN are consistently more dense than from rostral or caudal DCN in all the contralateral target nuclei. Finally, 5) it appears that the projection from the entire DCN to VB_l and the retinal projection (eye removal) to SC are in a further different category of density.

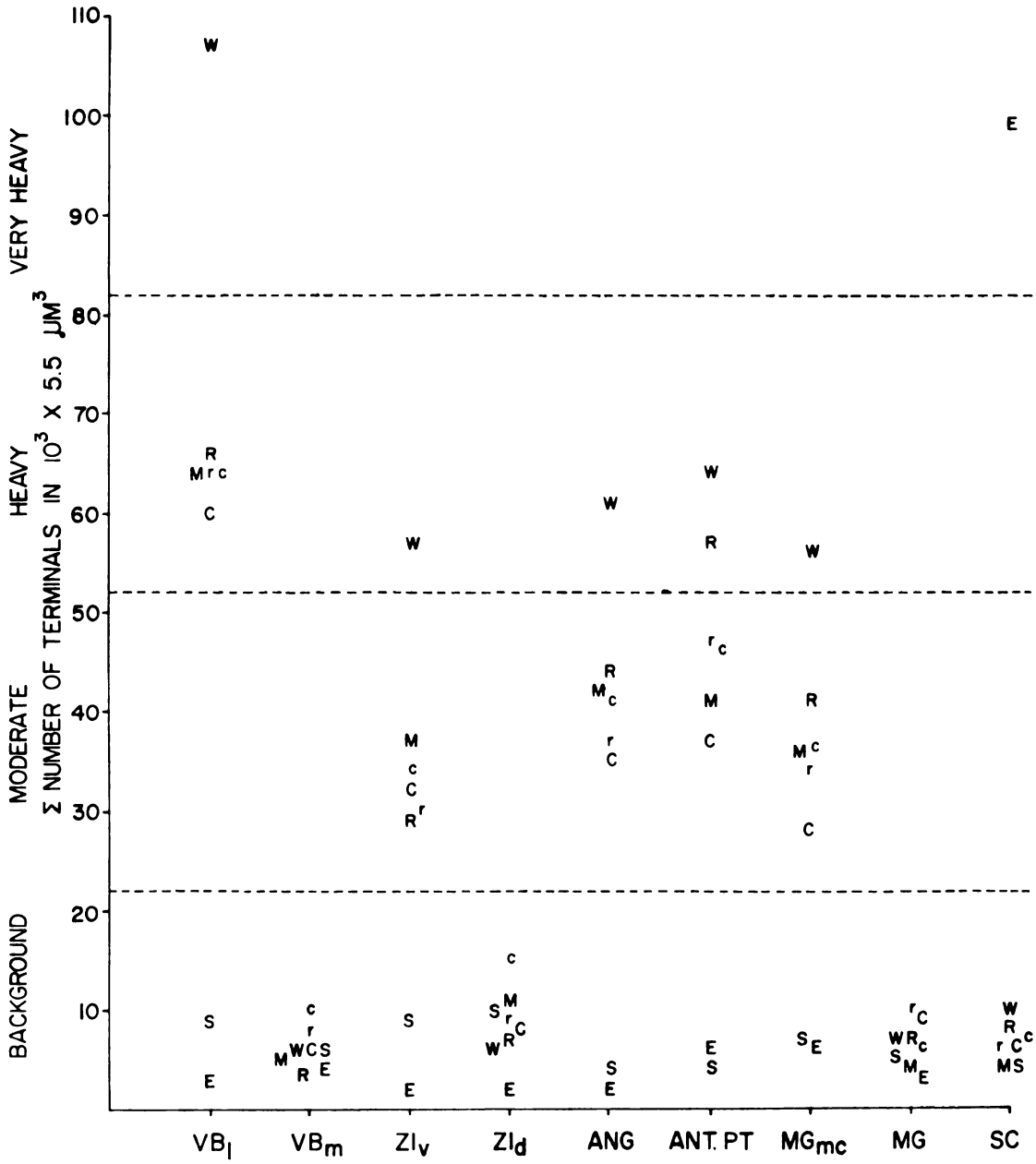
VERY HEAVY
HEAVY
MODERATE
BACKGROUND
Σ NUMBER OF TERMINALS IN 10^3 X 5.5 μM^3
110
100
90
80
70
60
50
40
30
20
10
VB$_l$
VB$_m$
ZI$_v$
ZI$_d$
ANG
ANT. PT
MG$_{mc}$
MG
SC

FIGURE 6

Figure 7. Density of terminal degeneration plotted as total number of silver grains in a volume of tissue (10^3 x 5.5 μm^3), from each of nine ipsilateral nuclei. Symbols same as in Figure 6.

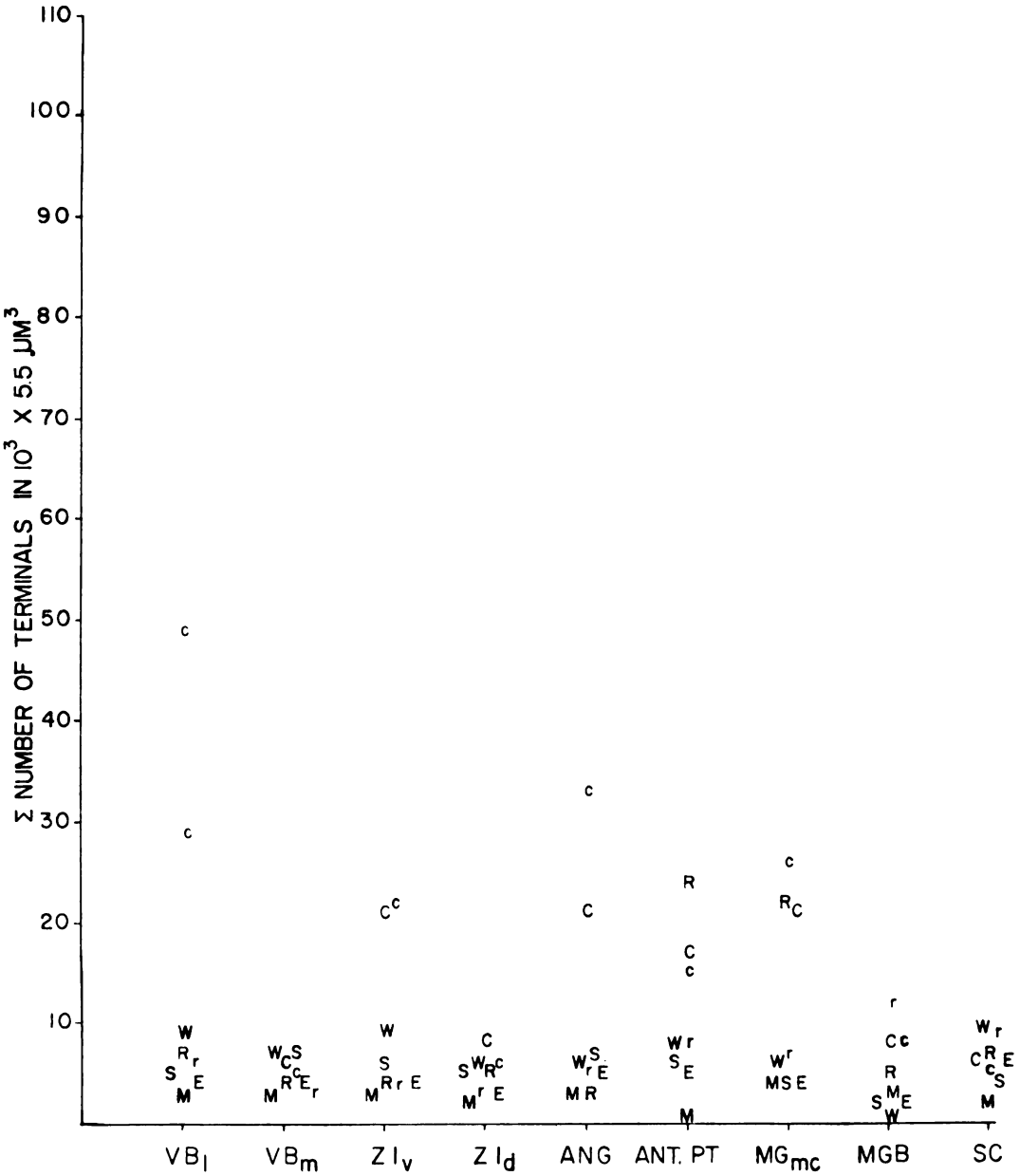
Σ NUMBER OF TERMINALS IN 10^3 X 5.5 μM^3
110
100
90
80
70
60
50
40
30
20
10
VB$_l$
VB$_m$
ZI$_v$
ZI$_d$
ANG
ANT. PT
MG$_{mc}$
MGB
SC

FIGURE 7

considered "heavy" in the extra-VB nuclei and "very heavy" in VB. To the latter category would also belong the degeneration in SC after eye removal.

Diencephalic Target Nuclei of DCN Projections

Ventrobasal Complex

Projections from the DCN to VB_l have been demonstrated in the opossum (Hazlett et al., '72; RoBards and Watkins, '75), hedgehog (Jane and Schroeder, '71), tree shrew (Schroeder and Jane, '71), rat (Lund and Webster, '67a; Basbaum et al., '77), cat (Matzke, '51; Hand and Liu, '66; Boivie, '71a; Jones and Burton, '74; Groenewegen et al., '75; Hand and Van Winkle, '77), raccoon (Welker and Johnson, '65), and macaque monkey (Walker, '38; Bowsher, '61). The pattern of termination is an "onion skin" type of somatotopic concentric laminae: gracile fibers terminating laterally, and cuneate fibers medially in the lateral division of VB (Welker and Johnson, '65; Lund and Webster, '67a; Boivie, '71a); and the medial division of VB receiving projections from the main sensory trigeminal nucleus (Lund and Webster, '67b; Smith '73). In this study, one caudal lesion ($RDCN_{53}$) encroached slightly on the other side damaging the nucleus of Bischoff (Figure 2) mostly where the tail is represented (Johnson et al., '68); ipsilateral degeneration resulted in VB_l, which was confined to a small area lateralmost in VB_l.

Hand and Van Winkle ('77) reported that lesions rostral to the obex produced less degeneration in VB_l in the cat than caudal lesions, even when the former were larger. Such a difference was not

found in this study: density of degeneration in VB_1 was similar in rostral and caudal cases, and so were the spatial dimensions of the area covered by the terminals. Degeneration was denser, however, when lesions involved the entire rostro-caudal extent of the DCN (Figure 6), and in all DCN lesions it was significantly ($p < .05$) denser in VB_1 than in other target nuclei.

Spinothalamic fibers terminate throughout the rostro-caudal extent of VB_1 in tree shrew (Schroeder and Jane, '71) and in primates (Mehler et al., '60; Mehler, '62 and '69). In the chimpanzee, macaque and man-but not in subprimates-Mehler described the terminals of fibers from the spinal anterolateral funiculus to VB_1 as occurring only in some cell clusters in what he called "bursts," overlapping with the DCN terminals in an "archipelago" fashion. A similar pattern of terminals in the macaque's VB_1 has also been reported for the ventral spinothalamic tract (Kerr '75). In the opossum, ascending afferents from all segments of the cord terminate in the most ventral part of VB (Hazlett et al., '72); and, in the hedgehog, no spinal fibers were found terminating in VB (Jane and Schroeder, '71). In the cat, spinothalamic fibers (except from the lateral cervical nucleus: LCN) do not terminate in VB_1 but in the ventral lateral nucleus and do not overlap with the DCN projection to VB (Boivie, '71b; Jones and Burton, '74); projections from the LCN, however, terminate throughout VB_1 but are concentrated dorsolaterally (Boivie, '70). In the rat, a spinothalamic projection has been described as terminating in the rostral third of VB, overlapping there with DCN terminals (Lund and Webster, '67b; Mehler, '69). Our

results are in agreement with such a description; degeneration from spinal hemisections at C_3-C_4 was present in VB_l in the most rostral two (levels A and B in Figure 4) of the levels where DCN terminals were found in VB (levels A to G). Lund and Webster ('67b) observed an additional field of degeneration in the caudolateral portion of VB_l, which occurred after high cervical cord hemisections (C_1-C_2) but not at C_3 or below; they attributed it to the LCN. The rat's homologue of an LCN, however, appears to extend throughout the segments of the cord (Gwyn and Waldron, '68).

Zona Incerta

A projection from DCN to zona incerta has been reported in the opossum (Hazlett et al., '72; RoBards and Watkins, '75), the hedgehog (Jane and Schroeder, '71), and the cat (Hand and Liu, '66; Hand and Van Winkle, '77). In the latter species, Boivie ('71a) described it as occupying the medial portion of ZI, while spinothalamic terminals (other than LCN's) occupied the lateral portion. In the rat, however, Lund and Webster ('67a) traced DCN fibers to the lateral part of ZI. A ventral division of ZI (ZI_v) has also been reported as the recipient of projections from the DCN in the hedgehog (in: Schroeder and Jane, '71), and from the principal sensory trigeminal nucleus in the rat (Smith, '73).

In the present study, terminal degeneration extended throughout the medio-lateral extent of the ventral region of ZI. More dorsally, there seemed to be a slight amount of degeneration, but when counted it did not rise significantly above the background (Figure 6),

and statistical analysis placed the dorsal region (ZI_d) in the non-target nuclei subset. At the most then, there may be a few scattered ML fibers terminating in ZI_d. The dorsal boundary of the degeneration in ZI_v however, varied slightly from section to section (Figure 4).

Review of the "PO" Region

Of the four diencephalic nuclei (Ang, Ant.Pt, MG_{mc}, ZI_v) which were identified in this study as a subset of extra-VB targets, three (Ang, Ant.Pt, and MC_{mc}) have often been included in a "PO" region. A "posterior nuclear group" was described in the cat by Rose and Woolsey ('58) as composed of the suprageniculate nucleus (Sg), the area extending anteriorly from the medial geniculate to VB, and MG_{mc} which they considered a differentiated portion of PO. Poggio and Mountcastle ('60) extended it to include the posterior nucleus of Rioch ('29) and the ventral portion of his lateral posterior nucleus (LP). They reported a heterogeneity of cellular characteristics in this zone (PO): some cells were found to be modality specific, responding only to auditory, vestibular, light mechanical, or noxious stimuli; other cells were found to be multimodal, responding to more than one stimulus modality. All somatic sensory responses were to bilateral stimulation, a fact they attributed to bilateral termination of afferents from the anterolateral column of the spinal cord. The bilaterality was also reported by Whitlock and Perl in the cat ('59) and monkey ('61); they, however, restricted their PO region to MG_{mc} and Sg. Furthermore, Poggio and Mountcastle ('60) believed

that DCN projections do not terminate in PO, but that their fibers "terminate wholly within VB."

Moore and Goldberg ('63) subdivided the PO region in the cat into: 1) a medial portion (PO_m) receiving afferents from the ascending somatic sensory pathways; and 2) a lateral portion (PO_l) which they described as an anterior extension of MG_{mc}, reaching dorsolaterally over the caudal end of VB and separating it from the external medullary lamina, and which received projections from the inferior colliculus. MG_{mc} was dealt with separately, apparently excluded from the PO group. In the rabbit, however, Tarlov and Moore ('66) could not identify a similar PO_l; instead, they referred to a PO homologous to the cat's PO_m, and equated the internal division of the medial geniculate (MG_i = MG_{mc}) with the cat's PO_l. And in the kangaroo rat, Carey and Webster ('71) did not identify a PO_l but instead, they described inferior colliculus projections to "medial posterior thalamic nuclei" and to "lateral posterior thalamic nuclei."

Jones and Powell ('68) further defined a "PO group" in the cat similar to that of Goldberg and Moore ('63), but added to it "adjacent portions of the pretectum" and the dorsal part of MGB. The dorsal lobe of MGB had previously been included in PO, but had been specifically mentioned only by Tarlov and Moore ('66) in the rabbit. Diamond et al., ('69) then subdivided the cat's PO_m into an intermediate PO (PO_i:between PO_m and PO_l) and a somewhat shrunken PO_m. While PO_l received afferents from the interior colliculus and from auditory neocortical areas AI and AII; PO_i received projections

from the lateral tegmental system and from the posterior ectosylvian, insulo-temporal, and suprasylvian fringe auditory areas of the neocortex. PO_m in the cat has also been subdivided by Berkley ('73) into: 1) an anterior portion (PO_m) between VB and the intralaminar nuclei, where few cells possessed wide peripheral receptive fields and displayed multimodal responses; and 2) a posterior portion (PO_p) composed of MG_{mc} and Sg, where many cells displayed such characteristics.

Some authors, however, have expressed discontent with the PO concept and its inconsistencies. Graybiel ('72) favored replacing the PO term and its subdivisions with Rose and Woolsey's "posterior nuclear group," and addressing nuclear entities such as dorsal MGB and Sg; she also relegated the rostral portion of PO_m back to the LP nucleus. And Jones and Burton ('74) dropped Sg and (most of) MG_{mc} from the PO group, but they retained the term and its PO_m, PO_l, and PO_i subdivisions. In the present study, discrete loci of degeneration were observed in the posterior region of the thalamus, they are best described in specific nuclei: nucleus angularis, the anterior pretectal nucleus, and the magnocellular division of the medial geniculate body.

Nucleus Angularis

A region composed of large and small cells, capping the dorsomedial aspect of VB and intercalated between VB_m and the central lateral nucleus (CL) was included by Poggio and Mountcastle ('60) in the cat's posterior nuclear group. This region which corresponds to

the ventral portion of Rioch's ('29) LP nucleus, has emerged as the major component of PO_m (Moore and Goldberg, '63; Diamond et al., '69; Boivie, '71a and b; Jones and Powell, '71; Berkley, '73); it appears to correspond to nucleus angularis of the present study.

Projections to this area (Ang or PO_m) in the cat have been reported from the DCN (Boivie, '71a; Jones and Powell, '71; Jones and Burton, '74; Hand and Van Winkle, '77), the spinothalamic pathway (Boivie, '71b; Jones and Powell, '71; Jones and Burton, '74), the lateral cervical nucleus (Boivie, '70), and neocortical areas SI and SII (Jones and Powell, '68 and '71).

In the opossum, Hazlett et al., ('72) described DCN, spinal and cerebellar (dentate and interposed nuclei) projections to a thalamic region they identified as the caudo-lateral portion of the ventral lateral nucleus of Oswaldo-Cruz and Rocha-Miranda ('67). Similar results were found by Walsh and Ebner ('73) who reported also "additional afferents from the ascending reticular formation." Killackey and Ebner ('72) expanded the area to include "nucleus C" of Oswaldo-Cruz and Rocha-Miranda ('67) and the central lateral nucleus. They named this expanded area "central intralaminar nucleus" (CIN). RoBards and Watkins ('75) then reported DCN projections in the opossum to CIN.

Mehler ('66) considered the caudal subdivision of Olszewski's ('52) central posterolateral nucleus (VPL_c) to be the primate homologue of PO. DeVito ('71) equated the suprageniculate nucleus (Sg) with PO in the macaque and squirrel monkey, and she reported that the descending somatic projections were to a region similar to the cat's

PO, which she then identified as oral pulvinar and the rostral part of medial pulvinar.

In the rat, the region was included in nucleus "lateralis thalami" by Gurdjian ('27). Lund and Webster ('67a and '67b) referred to it as "posterolateral complex, pars lateralis" (LPL), and reported that DCN and spinothalamic fibers terminate in a large-celled dorsal portion. Cowan et al., ('72) described a similar descending connection from the somatic sensory neocortex in the mouse, but they labelled the region "ventral lateral" (VL) nucleus. Mehler ('69) also found spinal and cerebellar projections to this area in the rat; he suggested that it corresponds to the lateral subdivision of nucleus angularis described by M. Rose ('35) in the rabbit, while its medial subdivision corresponds to the central lateral nucleus.

In the present study, the region in question has been identified as nucleus angularis (Figure 8), and terminal degeneration has been observed in it in all DCN lesions. The locus of degeneration moves to a slightly more ventral position at its caudalmost level (level H). Jones and Burton ('74) reported that in the cat, PO_m extends caudally to include a group of cells usually considered part of MG_{mc}. In the present study, loci of degeneration in the anterior pretectal nucleus and in MG_{mc} were separated from that in nucleus angularis by 450 to 600 μm in the anterio-posterior axis (Figures 4 and 5).

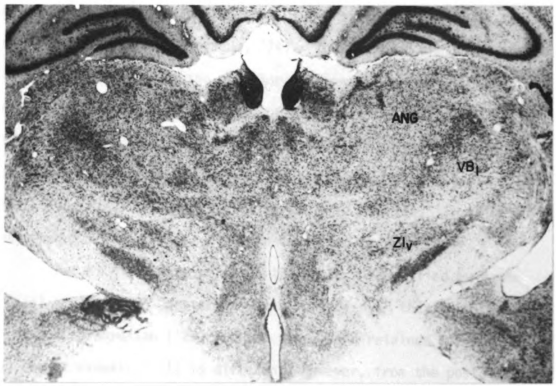

Figure 8. Coronal section through the diencephalon of the rat, at a level corresponding to level E (to F) of Figure 4; thionine stain.

Anterior Pretectal Nucleus

This is the largest of the pretectal nuclei in a variety of mammals including the rat (Figure 9) (Rose, '42; Scalia, '72); in the cat, however, it is much smaller and less clearly demarcated (Rose, '42), and the most prominent of the pretectal nuclei is the posterior (Kanaseki and Sprague, '74). The anterior pretectal nucleus (Ant.Pt) corresponds to the anterior portion of the pretectal nucleus and to the deep pretectal nucleus of Bucher and Nauta ('54). Unlike the other pretectal nuclei, Ant.Pt was found to be free of terminal degeneration following eye removal in a number of investigations in the rat and other species (Hayhow et al., '62; Scalia, '72; Kanaseki and Sprague, '74) and in control cases in the present study.

Ant.Pt also corresponds to the nucleus identified by Ramón y Cajal ('09-'11) as "posterior thalamic nucleus;" this label was also used by Gurdjian ('27) and has since been retained for rodents and "lower mammals." It is different, however, from the posterior nucleus described by Rioch ('29) which has been identified in the cat as inferior pulvinar, and shown to receive heavy projections from neocortical areas 17, 18, and 19, and the area of Clare-Bishop (Kanaseki and Sprague, '74; Kawamura el al., '74). Jones and Powell ('71) and Robertson and Rinvik ('73) considered the anterior pretectal nucleus identified by Berman ('68) in the cat to be nucleus limitans, and it was then included in the suprageniculate nucleus (Sg) by Diamond et al., ('69), and by Jones and Powell ('71).

Ramón y Cajal ('09-'11) first described collaterals from the "medial ribbon of Reil" (medial lemniscus) to the "posterior thalamic

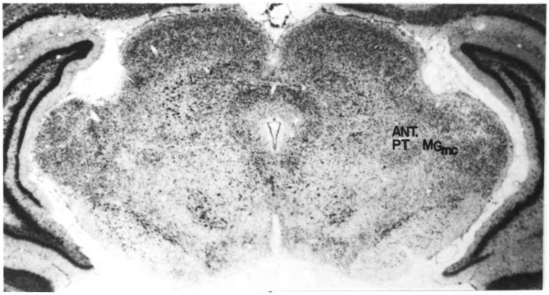

Figure 9. Coronal section through the diencephalon of the rat, at a level corresponding to level K of Figure 4; thionine stain.

nucleus" in the mouse. Hazlett et al., ('72) found a DCN projection to the oppossum's "pretectal nucleus," which is considered a homologue of the nucleus posterior thalami of Cajal (Oswaldo-Cruz and Rocha-Miranda, '67). Hand and Van Winkle ('77) reported cuneate projections to a supragenículate nucleus in the cat which probably included Ant. Pt. Jane and Schroeder ('71) illustrated terminal degeneration in the "pretectal nucleus" of the hedgehog following DCN lesions, but they did not discuss it. In the rat, Lund and Webster ('67a) described DCN projections to the ventral portion (pars reticularis: Scalia, '72) of the anterior pretectal nucleus; and Smith ('73) reported projections from the principal sensory trigeminal nucleus in the rat to a "posterior thalamic region" which he also referred to as "posterior thalamic nucleus," it appeared to involve a part of Ant.Pt. Libouban ('64) recorded from the anterior pretectal nucleus in the rat which she identified as "pretectal nucleus" or "posterior thalamic nucleus of Cajal;" she found that medium-sized elements (approximately 40% of the total population) were responsive to stimulation of the body surface and face and to displacement of the vibrissae. Davidson ('65) recorded from a "posterior nuclear complex" or "PO" in the rat; he reported a bilateral somatic representation with a rather poor topographical organization: a tendency of the hindleg and tail representation to be confined to a smaller lateral area. From his diagrams it would appear that this "posterior nuclear complex" mainly comprised the anterior pretectal nucleus, with some involvement of MG_{mc} and of Gurdjian's ('27) nucleus lateralis thalami.

In the present study, terminal degeneration was observed in the anterior pretectal nucleus. The degeneration was not confined to the ventral subdivision of the nucleus as previously reported (Lund and Webster, '67a), but it was uniformly present throughout its dorso-ventral extent. (It seemed more dense laterally.) It did not, however, extend to the rostral levels of the nucleus as deliminted by Scalia ('72), i.e., the anterior portion of the pretectal nucleus of Bucher and Nauta ('54) which Scalia included in Ant. Pt, did not have any degeneration in it.

Spinothalamic afferents to the "pretectal region" have been described in the macaque by Walker ('38). Also, in the macaque, squirrel monkey and chimpanzee, Mehler ('69) traced projections from the anterolateral funiculus of the spinal cord to what he suggested may be the "posterior pretectal nucleus." He had previously found a similar connection in man (Mehler, '62) and had identified the area as "nucleus posterior of Spalteholz." In the hedgehog, Jane and Schroeder ('71) illustrated spinal terminals in a "pretectal nucleus," and Lund and Webster ('67b) reported a spinal projection to (the ventral portion of) the anterior pretectal nucleus.

Corticofugal projections were reported in the cat, from the area of Clare-Bishop (in the lateral suprasylvian gyrus) and from areas 7 and 21 (of the middle suprasylvian gyrus) to the anterior pretectal nucleus (Kawamura et al., '74); and from all parietal areas to nucleus limitans (=Berman's Ant.Pt) (Robertson and Rinvik, '73). Projections from the somatic sensory neocortex have also been reported to the "pretectal region" in the macaque and squirrel monkey

(DeVito, '71); and to the "ventral pretectum" (Price and Webster, '72) and the posterior thalamic nucleus (Valverde, '61) in the rat.

Magnocellular Division of the Medial Geniculate

Afferents from the anterolateral funiculus of the spinal cord have been described to terminate in MG_{mc} in the monkey (Mehler et al., '60), and in man (Mehler, '62). In the latter, Mehler observed that only large cells in the dorsomedial region of MG_{mc} were involved. In the cat, Boivie ('71b) reported a dense projection from the anterolateral funiculus, relating to large cells in the medial part of MG_{mc}; Jones and Burton ('74), however, reported that although some degeneration was associated with the large cells located medially, most of the degeneration related to smaller more caudal cells belonging to PO_m. They suggested that "reports of spinal terminals in MG_{mc} proper result from failure to recognize the full extent of PO_m." Those caudally located PO_m cells occupy an area in the cat's thalamus (Figure 2 in: Jones and Powell, '71) similar to the ventral region of Ant.Pt in the rat. Projections to MG_{mc} were also reported from the spinal cord in the rat (MG_m: Lund and Webster, '67b), from the lateral cervical nucleus in the cat (Boivie, '70), and from the ventral spinothalamic tract in the macaque (Kerr, '75).

DCN and spinal fibers have been reported to terminate in the caudal portion of a posterior thalamic nucleus in the opossum (Hazlett et al., '72), which may be the small medial division of MGB identified by Morest ('65) in Golgi preparations in this animal.

DCN and spinal projections have also been described to a "PO complex" in the hedgehog (Jane and Schroeder, '71) and tree shrew (Schroeder and Jane, '71); this area appears closely ralated to MGB in the figures.

DCN fibers were reported terminating in MG_{mc} in the cat (Hand andLiu, '66; Hand and Van Winkle, '77). Boivie ('71a) however, did not observe them in MG_{mc}, and Jones and Burton ('74) were uncertain as to their termination there. In the rat, Lund and Webster ('67a) reported DCN projections to MG_{mc} ("MG_{m}"). In the present study DCN terminals were observed in MG_{mc}; they appeared related to both the large and small cells.

Smith ('73) reported a projection from the principal sensory trigeminal nucleus in the rat to a posterior thalamic region which included MG_{mc}. Fibers from nucleus caudalis of the trigeminal complex have also been reported to terminate in MG_{mc} in the rat (Lund and Webster, '67b), the cat (Stewart and King, '63), and marmoset (Dunn and Matzke, '68). However, Tiwari and King ('74) attributed this thalamic connection (in baboon and squirrel monkey) to a projection from the reticular nuclei adjacent to nucleus caudalis.

Ipsilateral Degeneration

RoBards and Watkins ('75) reported some degeneration in extra-VB target nuclei ipsilateral to the DCN lesion in the opossum. In the present study the degeneration in all the target nuclei was strictly contralateral to the DCN lesion; ipsilateral degeneration was only encountered when the lesion encroached on the other side,

as in some of the caudal lesions (Figure 2). However, in one case with a rostral DCN lesion confined to one side ($RDCN_{36}$), a light amount of degeneration was present in the ipsilateral Ant.Pt. and MG_{mc} (Figure 4). It may be due to a slight encroachment of the lesion on the inferior vestibular nucleus. Vestibular responses have been recorded from this thalamic region (Mickle and Ades, '54; Poggio and Mountcastle, '60; Wepsic, '66).

Other Nuclei

A DCN projection has been reported to the parafascicular nucleus (Pf) in the opossum (Hazlett et al., '72; RoBards and Watkins, '75). In the present study, degeneration was observed in Pf only occasionally, and a DCN projection to it cannot be ascertained.

A projection from the DCN has been reported to the deep layers of the superior colliculus in the opossum (Hazlett et al., '72; RoBards and Watkins, '75), rat (Lund and Webster, '67a), and cat (Hand and Liu, '66; Hand and Van Winkle, '77). Some degeneration was also observed in the present investigation, in the deep layers of the caudal levels of the superior colliculus, following DCN lesions.

Rostral and Caudal DCN Comparisons

Cytoarchitecture

Two different patterns of cytoarchitecture have been described by Kuypers and Tuerk ('64) in various regions of the dorsal column nuclei of the cat: 1) clusters composed of round cells with bushy and intertwined dendrites and whose perikarya are organized in

circles with cell-free cores. These clusters occupy the dorsal region of the DCN caudal to the obex. 2) Rostral to the obex, and in the ventral region caudal to it, the cells are triangular and multipolar and they are diffusely organized; they are of the radiating type, sparsely ramifying and starting to ramify closer to the soma then the clusters cells. Basbaum and Hand ('73) also described two cytoarchitectonic subdivisions in the rat's cuneate nucleus: 1) a region caudal to the obex made up of round cells arranged in "bricks," extending throughout the medio-lateral and dorso-ventral extents of the nucleus, except in its ventralmost aspect, and isolated from each other by fiber bundles; and 2) a region rostral to the obex, composed of round, spindle shaped and multipolar cells, and which does not display the "slab" architecture of the caudal region. This "slab" architecture, however, simply represents the "resorting zones" where the scrambled dorsal root fibers from various peripheral fields "become reshuffled" into fiber laminae to produce a somatotopic organization: in raccoons, and probably in other species as well, those "bricks" represent the digits of the forepaw (Johnson et al., '68).

Afferents

Neocortical descending projections to the DCN of the cat were reported to terminate mostly in the regions of diffuse cellular organization, while the cell clusters region received only few fibers from the cerebral neocortex (Kuypers and Tuerk, '64).

In addition to their main input from the primary fibers in the dorsal funiculus (from the dorsal roots), and to their corticofugal

afferents, the cuneate and gracile nuclei have been reported to receive fibers ascending in the lateral funiculus in the opossum (Hazlett et al., '72), and in the dorsolateral funiculus (DLF) in the cat (Gordon and Grant, '72). In the latter species, DLF fibers and non-primary fibers ascending in the dorsal funiculus have been found to terminate mainly in the regions of diffuse cytoarchitecture in the DCN (Rustioni, '73 and '74). The DLF projection to the gracile nucleus of the rat was also reported to terminate principally in the rostral portion (Tomasulo and Emmers, '72), and so was that to the cuneate and gracile nuclei in the macaque (Nijensohn and Kerr, '75).

Dorsal Roots Distribution

Dorsal root fibers in the cat were found to form dense terminal plexuses in relation to specific cell clusters, while in the region of diffuse cytoarchitecture, dorsal roots terminals were diffuse and displayed a greater intersegmental overlap than in the clusters regions (Kuypers and Tuerk, '64). This overlap was also greater in the rostral than in the caudal portions of the rat's DCN (Basbaum and Hand, '73).

Peripheral Receptive Fields

Gordon and Seed ('61) have reported that most of the cells in the rostral portion of the cat's gracile nucleus possess large peripheral fields (51.1cm^2), while those of the middle region displayed samll fields (4.5cm^2) and mutual inhibition. However, these characteristics are more understandable in terms of somatotopic organization: the large peripheral fields are from proximal parts of the

body, while the distal parts possess small peripheral fields and their DCN neurons display mutual inhibition. In addition, each particular receptive field is represented unchanged throughout its rostro-caudal representation in the DCN (Winter, '65; Johnson et al., '68).

Efferents

Some authors have identified more numerous diencephalic targets from the rostral DCN than from their other portions: Hand and Liu ('66) reported projections from the rostral gracile nucleus in the cat to MG_{mc}, the "posterior thalamic complex," the ventral posterolateral complex (VPL=VB_l), and ZI; while the middle portion of the gracile projected only to MG_{mc} and VPL. Hand and Van Winkle ('77) further observed in the cat that the rostral portion of the cuneate nucleus as well as its caudal portion and the ventral zone of its middle portion projected to the fields of Forel, MG_{mc}, PO_l, PO_m, Sg, VPL, and ZI; while the dorsal zone of its middle portion projected only to MG_{mc}, Sg, and VPL. They suggested that the former DCN regions represented a paleolemniscal system and the latter a neolemniscal system. In the rat, Lund and Webster ('67a) reported projections from the portion of the DCN rostral to the obex to the anterior pretectal nucleus, "lateral posterolateral complex" (LPL), MG_m (equivalent to MG_{mc}), VPL, and ZI; but only to MG_m and VPL from the DCN region caudal to the obex. However, similar diencephalic projections were reported from various rostro-caudal levels of the DCN in the opossum (Hazlett et al., '72; RoBards and Watkins, '75), and the hedgehog (Jane and

Schroeder, '71) and from the caudal and rostral portions of the DCN in the cat (Boivie, '71a).

In the present study, lesions rostral or caudal to the obex produced similar patterns of degeneration in the diencephalon: the same target nuclei were involved, the amount of degeneration was similar in the various nuclei in rostral and caudal cases and the terminals extended over virtually identical antero-posterior, dorso-ventral, and medio-lateral dimensions in the particular nuclei in rostral and in caudal lesions. Lesions including the entire DCN produced denser degeneration in all the target nuclei but did not affect its spatial extents within the nuclei. It is possible that a lesion restricted to the dorsal portion of the DCN caudal to the obex could have produced a different pattern. However, the quantitative results obtained argue against such a possiblity: if the dorsal portion of the caudal DCN had restricted diencephalic projections, the total amount of degenerating terminals in the various target nuclei resulting from caudal DCN lesions would have been smaller than that resulting from rostral DCN lesions.

Overview of Rostral and Caudal DCN Differences

Cells throughout the gracile nucleus of the cat were fired by antidromic stimulation of the medial lemniscus (Gordon and Seed, '61). Injections of HRP in the cat's thalamus extending over VB and portions of most of the extra-VB targets produced labelling in the clusters cells but also in the multipolar and triangular cells of the other DCN regions (Berkley, '75; Cheek et al., '75). However,

40% of the cells in the rostral gracile region did not respond to antidromic stimulation in the medial lemniscus (Gordon and Seed, '61), and some DCN cells remained unlabelled after the thalamic HRP injections, particularly small cells in the rostral region (Berkley, '75; Cheek et al., '75). These cells may have other projections, for example, to the inferior olive as suggested by Berkley ('75) or to the cerebellum where HRP injections in the anterior lobe labelled cells in the rostral DCN (Cheek et al., '75). However, at least some of the cerebellar projections are collaterals of fibers in the medial lemniscus (ML): Gordon and Seed ('61) reported that some gracile units in the cat responded to antidromic stimulation in both the cerebellum and the medial lemniscus; and Johnson et al., ('68) described large cells in the M-T area of the cuneate, which responded to deep stimulation only, and atrophied only after lesions of both the cerebellum and the medial lemniscus. It is also probable that the small cells in the DCN which remain unlabelled after thalamic HRP injections and which do not respond to ML antidromic stimulation are interneurons: they may be the units responding trans-synaptically to ML antidromic stimulation (Gordon and Seed, '61), and they may be the recipients of the corticofugal projections to the DCN, of fibers from the dorsolateral funiculus and of non-primary afferents from the dorsal funiculus. These interneurons may be scattered throughout the DCN but concentrated in the rostral region.

In summary, the DCN in the rat projects to a number of discrete nuclear regions in the thalamus and subthalamus; they include:

the ventrobasal complex (pars lateralis), nucleus angularis, the anterior pretectal nucleus, the magnocellular division of the medial geniculate, and the ventral part of the zona incerta. No differences were observed in the present study in diencephalic projections from rostral and caudal DCN. The difference between DCN regions rostral to the obex and DCN regions caudal to it may only be in a preferential concentration of interneurons rostrally, and/or in additional brainstem projections from the rostral portion.

BIBLIOGRAPHY

BIBLIOGRAPHY

Basbaum, A. I. and P. J. Hand 1973 Projections of cervicothoracic dorsal roots to the cuneate nucleus of the rat, with observations on cellular "bricks." J. Comp. Neur., 148, 347-360.

Basbaum, A. I., G. J. Giesler and D. Menetrey 1977 Medullo-thalamic projections in the rat. Anat. Rec., 187, 531.

Berkley, K. J. 1973 Response properties of cells in ventrobasal and posterior group nuclei of the cat. J. Neurophysiol., 36, 940-952.

Berkley, K. J. 1975 Different targets of different neurons in nucleus gracilis of the cat. J. Comp. Neur., 163, 285-304.

Berman, A. L. 1968 The Brain Stem of the Cat. A Cytoarchitectonic Atlas with Stereotaxic Coordinates. The University of Wisconsin Press, Madison.

Boivie, J. 1970 The termination of the cervicothalamic tract in the cat. An experimental study with silver impregnation methods. Brain Res., 19, 333-360.

Boivie, J. 1971 The termination in the thalamus and the zona incerta of fibres from the dorsal column nuclei (DCN) in the cat. An experimental study with silver impregnation methods. Brain Res., 28, 459-490. (a)

Boivie, J. 1971 The termination of the spinothalamic tract in the cat. An experimental study with silver impregnation methods. Exp. Brain Res., 12, 331-353. (b)

Bowsher, D. 1961 The termination of secondary somatosensory neurons within the thalamus of Macaca mulatta: an experimental degeneration study. J. Comp. Neur., 117, 213-228.

Bucher, V. M. and W. J. H. Nauta 1954 A note on the pretectal cell groups in the rat's brain. J. Comp. Neur., 100, 287-295.

Carey, C. L. and D. B. Webster 1971 Ascending and descending projections of the inferior colliculus in the kangaroo rat (Dipodomys merriami). Brain, Behav. Evol., 4, 401-412.

Cheek, M. D., A. Rustioni and D. L. Trevino 1975 Dorsal column nuclei projections to the cerebellar cortex in cats as revealed by the use of the retrograde transport of horseradish peroxidase. J. Comp. Neur., 164, 31-46.

Cowan, W. M., D. I. Gottlieb, A. E. Hendrickson, J. L. Price and T. A. Woolsey 1972 The autoradiographic demonstration of axonal connections in the central nervous system. Brain Res., 37, 21-51.

Davidson, N. 1965 The projection of afferent pathways on the thalamus of the rat. J. Comp. Neur., 124, 377-390.

DeVito, J. L. 1971 Corticothalamic connections of suprasylvian cortex in monkey. Exp. Neurol., 32, 489-501.

Diamond, I. T., E. G. Jones and T. P. S. Powell 1969 The projection of the auditory cortex upon the diencephalon and brain stem in the cat. Brain Res., 15, 305-340.

Dunn, J. D. and H. A. Matzke 1968 Efferent fiber connections of the marmoset (Oedipomidas oedipus) trigeminal nucleus caudalis. J. Comp. Neur., 133, 429-438.

Fink, R. P. and L. Heimer 1967 Two methods for selective silver impregnation of degenerating axons and their synaptic endings in the central nervous system. Brain Res., 4, 369-374.

Gordon, G. and G. Grant 1972 Afferents to the dorsal column nuclei from the dorsolateral funiculus of the spinal cord. Acta Physiol. Scand., 84, 30A-31A.

Gordon, G. and W. A. Seed 1961 An investigation of nucleus gracilis of the cat by antidromic stimulation. J. Physiol., Lond., 155, 589-601.

Graybiel, A. M. 1972 Some ascending connections of the pulvinar and nucleus lateralis posterior of the thalamus in the cat. Brain Res., 44, 99-125.

Groenewegen, H. J., A. J. P. Boesten and J. Voogd 1975 The dorsal column nuclear projections to the nucleus ventralis posterior lateralis thalami and the inferior olive in the cat: an autoradiographic study. J. Comp. Neur., 162, 505-518.

Gurdjian, E. S. 1927 The diencephalon of the albino rat. Studies on the brain of the rat. No. 2. J. Comp. Neur., 43, 1-114.

Gwyn, D. C. and H. A. Waldron 1968 A nucleus in the dorsolateral funiculus of the spinal cord of the rat. Brain Res., 10, 342-351.

Hand, P. and C. N. Liu 1966 Efferent projections of the nucleus gracilis. Anat. Rec., 154, 353-354.

Hand, P. J. and T. Van Winkle 1977 The efferent connections of the feline nucleus cuneatus. J. Comp. Neur., 171, 83-109.

Hayhow, W. R., A. Sefton and C. Webb 1962 Primary optic centers of the rat in relation to terminal distribution of the crossed and uncrossed optic nerve fibers. J. Comp. Neur., 118, 295-321.

Hazlett, J. C., R. Dom and G. F. Martin 1972 Spino-bulbar, spinothalamic and medial lemniscal connections in the American opossum, Didelphis marsupialis virginiana. J. Comp. Neur., 146, 95-118.

Heimer, L. 1970 Selective silver-impregnation of degenerating axoplasm. In: W. J. H. Nauta and S. O. E. Ebbesson (Eds.), Contemporary Research Methods in Neuroanatomy. Springer-Verlag, New York, pp. 106-131.

Jane, J. A. and D. M. Schroeder 1971 A comparison of dorsal column nuclei and spinal afferents in the European hedgehog (Erinaceus europeaus). Exp. Neurol., 30, 1-17.

Johnson, Jr., J. I., W. I. Welker and B. H. Pubols, Jr. 1968 Somatotopic organization of raccoon dorsal column nuclei. J. Comp. Neur., 132, 1-44.

Jones, E. G. and T. P. S. Powell 1968 The projection of the somatic sensory cortex upon the thalamus in the cat. Brain Res., 10, 369-391.

Jones, E. G. and T. P. S. Powell 1971 An analysis of the posterior group of thalamic nuclei on the basis of its afferent connections. J. Comp. Neur., 143, 185-216.

Jones, E. G. and H. Burton 1974 Cytoarchitecture and somatic sensory connectivity of thalamic nuclei other than the ventrobasal complex in the cat. J. Comp. Neur., 154, 395-432.

Kanaseki, T. and J. M. Sprague 1974 Anatomical organization of pretectal nuclei and tectal laminae in the cat. J. Comp. Neur., 158, 319-338.

Kawamura, S., J. M. Sprague and K. Niimi 1974 Corticofugal projections from the visual cortices to the thalamus, pretectum and superior colliculus in the cat. J. Comp. Neur., 158, 339-362.

Kerr, F. W. L. 1975 The ventral spinothalamic tract and other ascending systems of the ventral funiculus of the spinal cord. J. Comp. Neur., 159, 335-356.

Killackey, H. P. and F. F. Ebner 1972 Two different types of thalamocortical projections to a single cortical area in mammals. Brain Behav. Evol., 6, 141-169.

Kuypers, H. G. J. M. and J. D. Tuerk 1964 The distribution of the cortical fibres within the nuclei cuneatus and gracilis in the cat. J. Anat., Lond., 98, 143-162.

Libouban, S. 1964 Etude éléctrophysiologique des structures cérébrales du rat blanc. Comparaison avec les structures homologues du chat et du singe. Thèses, Univ. de Paris, pp. 1-99.

Lund, R. D. and K. E. Webster 1967 Thalamic afferents from the dorsal column nuclei. An experimental anatomical study in the rat. J. Comp. Neur., 130, 301-312. (a)

Lund, R. D. and K. E. Webster 1967 Thalamic afferents from the spinal cord and trigeminal nuclei. An experimental anatomical study in the rat. J. Comp. Neur., 130, 313-328. (b)

Matzke, H. A. 1951 The course of the fibers arising from the nucleus gracilis and cuneatus of the cat. J. Comp. Neur., 94, 439-452.

Mehler, W. R. 1962 The anatomy of the so-called "pain tract" in man: an analysis of the course and distribution of the ascending fibers of the fasciculus anterolateralis. In: J. D. French and R. W. Porter (Eds.), Basic Research in Paraplegia. Charles C. Thomas, Springfield, Ill., pp. 26-55.

Mehler, W. R. 1966 The posterior thalamic region in man. Confin. Neurol., 27, 18-29.

Mehler, W. R. 1969 Some neurological species differences--A posteriori. In: Comparative and Evolutionary Aspects of the Vertebrate Central Nervous System. Ann. N. Y. Acad. Sci., 167, pp. 424-468.

Mehler, W. R., M. E. Feferman and W. J. H. Nauta 1960 Ascending axon degeneration following anterolateral cordotomy. An experimental study in the monkey. Brain, 83, 718-750.

Mickle, W. A. and H. W. Ades 1954 Rostral projection pathway of the vestibular system. Amer. J. Physiol., 176, 243-246.

Moore, R. Y. and J. M. Goldberg 1963 Ascending projections of the inferior colliculus in the cat. J. Comp. Neur., 121, 109-135.

Morest, D. K. 1965 Identification of homologous neurons in the posterolateral thalamus of cat and Virginia opossum. Anat. Rec., 151, 390.

Nijensohn, D. E. and F. W. L. Kerr 1975 The ascending projections of the dorsolateral funiculus of the spinal cord in the primate. J. Comp. Neur., 161, 459-470.

Olszewski, J. 1952 The Thalamus of the Macaca Mulatta. S. Karger, Basel.

Oswaldo-Cruz, E. and C. E. Rocha-Miranda 1967 The diencephalon of the opossum in stereotaxic coordinates. I. The epithalamus and dorsal thalamus. J. Comp. Neur., 129, 1-38.

Poggio, G. F. and V. B. Mountcastle 1960 A study of the functional contributions of the lemniscal and spinothalamic systems to somatic sensibility. Johns Hopkins Med. J., 106, 266-316.

Price, T. R. and K. E. Webster 1972 The cortico-thalamic projection from the primary somatosensory cortex of the rat. Brain Res., 44, 636-640.

Ramón y Cajal, S. 1909-1911 (1955) Histologie du Système Nerveux de l'Homme et des Vertébrés. Paris, Maloine, Vol. II, pp. 407-409.

Rioch, D. McK. 1929 Studies on the diencephalon of carnivora. Part I. The nuclear configuration of the thalamus, epithalamus, and hypothalamus of the dog and cat. J. Comp. Neur., 49, 1-119.

RoBards, M. J. and D. W. Watkins 1975 Efferent projections of the dorsal column nuclei and the overlying dorsal columns of the Virginia opossum. Neurosci. Abstracts, N. Y., 1, 215.

Robertson, R. T. and E. Rinvik 1973 The corticothalamic projections from parietal regions of the cerebral cortex. Experimental degeneration studies in the cat. Brain Res., 51, 61-79.

Rose, J. E. 1942 The thalamus of the sheep: cellular and fibrous structure and comparison with pig, rabbit and cat. J. Comp. Neur., 77, 469-523.

Rose, J. E. and C. N. Woolsey 1958 Cortical connections and functional organization of the thalamic auditory system of the cat. In: H. F. Harlow and C. N. Woolsey (Eds.), Biological and Biochemical Bases of Behavior. University of Wisconsin Press, Madison, pp. 127-150.

Rose, M. 1935 Das Zwischenhirn des Kaninchens. Mém. de l'Acad. Pol. des Sci. et Lett., Cracovie, sér. B, 1-108.

Rustioni, A. 1973 Non-primary afferents to the nucleus gracilis from the lumbar cord of the cat. Brain Res., 51, 81-95.

Rustioni, A. 1974 Non-primary afferents to the cuneate nucleus in the brachial dorsal funiculus of the cat. Brain Res., 75, 247-259.

Scalia, F. 1972 The termination of retinal axons in the pretectal region of mammals. J. Comp. Neur., 145, 223-258.

Schroeder, D. M. and J. A. Jane 1971 Projection of dorsal column nuclei and spinal cord to brainstem and thalamus in the tree shrew, Tupaia glis. J. Comp. Neur., 142, 309-350.

Smith, R. L. 1973 The ascending fiber projections from the principal sensory trigeminal nucleus in the rat. J. Comp. Neur., 148, 423-446.

Stewart, W. A. and R. B. King 1963 Fiber projections from the nucleus caudalis of the spinal trigeminal nucleus. J. Comp. Neur., 121, 271-286.

Tarlov, E. C. and R. Y. Moore 1966 The tecto-thalamic connections in the brain of the rabbit. J. Comp. Neur., 126, 403-422.

Tiwari, R. K. and R. B. King 1974 Fiber projections from trigeminal nucleus caudalis in primate (squirrel monkey and baboon). J. Comp. Neur., 158, 191-206.

Tomasulo, K. C. and R. Emmers 1972 Activation of neurons in the gracile nucleus by two afferent pathways in the rat. Exp. Neurol., 36, 197-206.

Valverde, F. 1961 Conexiones corticotalámicas y corticopretectales. (Estudio experimental en la rata albina). Anal. de Anat., Granada, 10, 345-359.

Walker, A. E. 1938 (1966) The Primate Thalamus. The University of Chicago Press, Chicago.

Walsh, T. M. and F. F. Ebner 1973 Distribution of cerebellar and somatic lemniscal projections in the ventral nuclear complex of the Virginia opossum. J. Comp. Neur., 147, 427-446.

Welker, W. I. and J. I. Johnson 1965 Correlation between nuclear morphology and somatotopic organization in ventrobasal complex of the raccoon's thalamus. J. Anat., Lond., 99, 761-790.

Wepsic, J. G. 1966 Multimodal sensory activation of cells in the magnocellular medial geniculate nucleus. Exp. Neurol., 15, 299-318.

Whitlock, D. G. and E. R. Perl 1959 Afferent projections through ventrolateral funiculi to thalamus of cat. J. Neurophysiol., 22, 133-148.

Whitlock, D. G. and E. R. Perl 1961 Thalamic projections of spinothalamic pathways in monkey. Exp. Neurol., 3, 240-255.

Winer, B. J. 1962 Statistical Principles in Experimental Design. McGraw-Hill, New York.

Winter, D. L. 1965 N. gracilis of cat. Functional organization and corticofugal effects. J. Neurophysiol., 28, 48-70.

APPENDICES

APPENDIX A

FINK-HEIMER TECHNIQUE

APPENDIX A

FINK-HEIMER TECHNIQUE

A. Cut frozen sections at 30 μm and place them in 3% formalin.

B. Preliminary:

1. Maximum 4 sections (rat brain size) in each crucible

2. Wash in DW (dist. water) #1	3-5 mn
Wash in DW #2	3-5 mn
(Wash in DW #3)	
3. Potassium permanganate (0.05%) agitate frequently	5-20 mn
4. Wash in DW	
5. Oxalic acid (1%) Hydroquinone (1%) 1:1 ratio	1 mm or less until decolorized
6. Wash in DW #1	3 mn
Wash in DW #2	3 mn
Wash in DW #3	3 mn

C. Impregnation:

1. 0.5% Uranyl nitrate 88 ml 2.5% Silver nitrate 99 ml	1 hr. or more
2. 0.5% Uranyl nitrate 80 ml 2.5% Silver nitrate 120 ml	30-60 mn
3. Wash in DW #1	3 mn
Wash in DW #2	3 mn
Wash in DW #3	3 mn

D. Exposure: Ammoniacal silver
agitate constantly — 2-4 mn

1st Ammonium hydroxide (conc.) 4.2-4.4 ml
2nd Sodium hydroxide 5.4 ml
mix well
3rd Silver nitrate (2.5%) 90 ml
pour slowly
mix well

E. Developing:

Reducer	54 ml	1% citric acid
	54 ml	10% formalin
	180 ml	100% alcohol
	1600 ml	DW

1. 3 reducer changes	#1	2-5 sec
	#2	15 sec
	#3	45 sec-2 mn
2. Wash in DW		1 mn

F. Fixing:

1. Sodium thiosulfate (1%)	30 sec
2. Wash in DW #1	3-5 mn
Wash in DW #2	3-5 mn
Wash in DW #3	3-5 mn

G. Mount in Albrecht's alcohol gelatin

1.5% aqueous gelatin
80% alcohol 1:1 ratio

H. Dry at room temperature, or for 10-30 mn at 58°C

I. Dehydration: 5-10 mn in each

1. 70% alcohol
2. 95% alcohol
3. 100% alcohol
4. 100% alcohol
5. Xylene #1
6. Xylene #2

J. Coverslip

APPENDIX B

INSTRUCTIONS FOR COUNTING TERMINAL DEGENERATION

APPENDIX B

INSTRUCTIONS FOR COUNTING TERMINAL DEGENERATION

1. The counting I need you to do is to cross-check the one I did.

2. First, be careful not to move the table; and do not, at any time, move the eyepiece: it would move the ocular micrometer, and would change the area we are counting from.

3. There is a grid (an ocular micrometer) in the eyepiece; its upper left hand-side quadrant has 16 squares in it; we are going to count grains in 6 (random) of them; we are numbering the squares from left to right, top row first.

4. Move the fine focus knob so that the section gets slightly out of focus one way, then in focus, then slightly out of focus the other way; and count all the round black grains you will see. Look throughout the squares and check their corners too. If a grain is on the boundary line of the square, count it if it protrudes at all inside, even if most of it is outside. Do not count line-like things even if they are tiny; and make sure the grains you count are black, not dark gold or brown.

5. Count as "coarse," the grains that are half the size or larger of a (or: of this) nucleolus; when less than half its size, count them as "small."

   * Counting the grains as "coarse" and "small" helped prevent overlooking the smaller fibers especially when there were many large ones.

6. Do not count from strings of black grains or from series of stubby lines.

If "dust" was observed (occasionally), additional instructions were given:

You may see a "carpet" of fine grains uniformly distributed throughout the section (or most of it); you can still see them when the section is totally out of focus and blurred. Those are not terminals, do not count them.

APPENDIX C

COUNTS OF "GRAINS" OF TERMINAL DEGENERATION

Appendix Table C1.

Counts of silver grains of terminal degeneration in nine diencephalic nuclei resulting from rostral DCN lesions, caudal DCN lesions, entire DCN, and mixed rostral and caudal DCN lesions, and control lesions (eye removal, and sham DCN lesion).

Letters: R, r, C, c, W, M. E, and S are the abbreviations used in Figures 6 and 7.

In each lesion case, the contralateral counts (contra.), ipsilateral counts (ipsi.), and contralateral counts made by the judges, were all on the same section (section 1) for the particular nucleus.

Counts were also made on a second section in the five contralateral target nuclei (contra. in section:2). Those contralateral counts from two sections were added and averaged (M). The average was used in Figure 6, but all the counts used in the analyses of variance were from section 1 only.

APPENDIX C

COUNTS OF "GRAINS" OF TERMINAL DEGENERATION

	nuclei	Contra. in section: 1	2	M	Ipsi in section 1	Judges Contra Section 1
Rostral DCN lesion (R) ($RDCN_{34}$)	Ang	48	40	44	3	47
	Ant.Pt	59	54	57	24	61
	MG_{mc}	44	37	41	22	43
	VB_l	75	56	66	7	73
	ZI_v	32	25	29	4	31
	MGB	7			5	8
	SC	8			7	8
	VB_m	6			4	6
	ZI_d	7			5	7

	nuclei	Contra. in section: 1	2	M	Ipsi in section 1	Judges Contra Section 1
Rostral DCN lesion (r) $RDCN_{36}$)	Ang	39	34	37	5	43
	Ant.Pt	45	49	47	8	47
	MG_{mc}	36	32	34	7	
	VB_l	89	39	64	6	
	ZI_v	33	26	30	4	33
	MGB	10			12	
	SC	6			9	6
	VB_m	8			3	9
	ZI_d	9			3	

Caudal DCN lesion (C) ($RDCN_{53}$)	Ang	37	32	35	21	38
	Ant.Pt	41	32	37	17	43
	MG_{mc}	32	24	28	21	29
	VB_l	67	53	60	29	66
	ZI_v	40	23	32	21	38
	MGB	9			8	8
	SC	6			6	
	VB_m	6			6	
	ZI_d	8			8	

Caudal DCN lesion (c) ($RDCN_{61}$)		48	34	41	33	47
		45	46	46	25	43
		41	31	36	26	45
		79	48	64	49	73
		43	24	34	22	
		6			8	
		7			5	
		10			5	
		15			6	

	nuclei	Contra. in section: 1	2	M	Ipsi in section 1	Judges Contra Section 1
Entire DCN lesion (W) ($RDCN_{17}$)	Ang	71	51	61	6	
	Ant.Pt.	67	61	64	8	
	MG_{mc}	54	57	56	6	
	VB_l	120	94	107	9	
	ZI_v	56	57	57	9	
	MGB	7			5	
	SC	10			4	
	VB_m	6			7	
	ZI_d	6			6	

		Contra. in section: 1	2	M	Ipsi in section 1	Judges Contra Section 1
Mixed DCN lesion (M) ($RDCN_8$)		47	36	42	3	
		39	42	41	1	
		38	33	36	4	
		88	40	64	3	
		40	34	37	3	
		4			3	
		4			2	
		5			3	
		11			2	

Control: Eye removal (E) (RE_2)	Ang	2	5	
	Ant.Pt	6	5	7
	MG_{mc}	6	4	
	VB_l	3	4	
	ZI_v	2	4	
	MGB	3	2	
	SC	99	6	
	VB_m	4	4	
	ZI_d	2	3	

Control: Sham DCN lesion (S) ($RDCN_{37}$)	4	7	
	4	6	
	7	4	
	9	5	
	9	6	
	5	2	
	5	4	
	6	7	
	10	5	